Investigation of Urinary Proteome Alterations in a DEN-Induced Rat Model of Hepatic Inflammation-Cancer

Authors: Wang Yunlong, Gao Youhe, Youhe Gao

Date: 2022-01-09T17:45:29+00:00

Abstract

[Objective] To observe the dynamic changes in the urinary proteome across different disease stages in a DEN-induced inflammation-cancer model of hepatocellular carcinoma. Methods In this study, a rat inflammation-cancer model of hepatocellular carcinoma was established via intraperitoneal injection of DEN. Urine was collected weekly, differential proteins were identified by liquid chromatography-tandem mass spectrometry (LC-MS/MS), biological pathway analysis of differential proteins was performed using IPA software, and changes in urinary proteins at different disease stages were observed. Results Through DEN induction, 15 experimental rats developed different stages of the disease model from hepatitis to cirrhosis to hepatocellular carcinoma, with each rat exhibiting different rates of disease progression due to individual differences. Each rat displayed numerous differential proteins at different disease time points, and the differential proteins from different rats were all enriched in the same biological pathways related to liver injury, inflammatory lesions, tumorigenesis, and potential therapeutic targets for tumors. [Discussion] We can observe distinct changes in the urinary proteome at various stages of the inflammation-cancer model, and different rats exhibit different rates of disease progression due to individual differences, which suggests that we need to pay greater attention to individualized and precise detection in the future.

Full Text

Abstract

Objective: To investigate the dynamic changes in the urinary proteome across different stages of disease progression in a diethylnitrosamine (DEN)-induced rat model of inflammation-to-cancer transition.

Methods: We established a rat liver cancer-inflammatory cancer model through intraperitoneal injection of DEN and collected urine samples weekly. Differential proteins were identified using liquid chromatography-tandem mass spectrometry (LC-MS/MS), and biological pathway analysis of these proteins was performed using IPA software to observe urinary protein changes at different disease stages.

Results: Fifteen experimental rats were induced with DEN to develop various stages of hepatitis-cirrhosis-liver cancer. Individual rats exhibited different disease progression rates due to biological variation. Each rat showed numerous differential proteins at different time points, and these proteins were enriched in common biological pathways related to liver injury, inflammatory lesions, tumor development, and potential therapeutic targets.

Discussion: We observed distinct urinary proteome changes at each stage of the liver cancer-inflammatory cancer model. The individual variation in disease progression among different rats suggests the need for greater emphasis on personalized and precise detection strategies in future research.

Keywords: Proteomics; Urine; Inflammatory cancer model; Liver cancer

Introduction

Urine, formed through blood filtration and not subject to homeostatic regulation, accumulates various changes expelled by the body to maintain stability. Consequently, urine reflects physiological changes more rapidly and sensitively than blood, making it an important source for mining early disease biomarkers [1,2]. Previous studies have identified significant differential proteins in urine for conditions including pulmonary fibrosis [3], astrocytoma [3], pancreatic cancer [4], and bladder cancer [5]. Additionally, urine offers the advantages of non-invasive collection, large sample volumes, and continuous sampling. Therefore, we consider urine to be an excellent biological source for biomarker discovery. Animal models can exclude numerous complex confounding factors, minimizing their influence [6]. DEN-induced hepatocarcinogenesis differs from direct tumor modeling through cancer cell inoculation by simulating the stepwise human progression from hepatitis to cirrhosis to liver cancer, making it more practically significant for identifying early human liver cancer markers.

Liver cancer is a highly common malignant tumor with an insidious onset and rapid progression, yet relatively high incidence and mortality rates [7]. It occurs worldwide, with 626,000 new cases and 589,000 deaths annually, ranking as the sixth most common tumor globally and third in cancer-related mortality [8]. This demonstrates that liver cancer seriously threatens human health and life. China is among the countries with high liver cancer incidence, with approximately 100,000 deaths from primary liver cancer each year. Globally, 80% of liver cancer cases are directly related to infection-induced occult hepatitis and chronic viral hepatitis, leading to liver inflammation, fibrosis, and regenerative nodules [9]. Therefore, early diagnosis and treatment are crucial for improv-

ing survival in liver cancer patients. As the third leading cause of cancer death and lacking effective treatment measures, preventing liver cancer occurrence has become a major challenge.

Diethylnitrosamine, a nitrosamine compound, is not only a potent chemical carcinogen but also a common food contaminant found in food, cosmetics, beer, and cigarettes. Using DEN to induce liver cancer models allows determination of the timing of each stage of hepatocarcinogenesis and precancerous lesions, providing a reliable carcinogenesis model.

In this study, we constructed a rat liver cancer-inflammatory cancer model, collected urine weekly, and performed blood collection and tissue sampling at different time points. Blood biochemical indicators and liver tissue HE staining were used to determine pathological progression. Mass spectrometry analysis of collected urine samples was conducted to investigate changes in the urinary proteome and related biological pathways during disease progression, providing clues and a basis for clinical diagnosis and therapeutic target identification in liver cancer.

Methods

Animal Model and Sample Collection

Twenty male Wistar rats weighing 180g were purchased from Beijing Vital River Laboratory Animal Technology Co., Ltd. Rats received weekly intraperitoneal injections of DEN at a dose of 50mg/kg and were housed under standard conditions with a 12-hour light-dark cycle, temperature of 22℃$±$1℃, and humidity of 65%-70%. Urine was collected weekly. Blood liver function tests and liver tissue HE sections were performed before injection (week 0) and at weeks 4, 12, 16, and 18 post-injection to evaluate model progression. All experimental procedures complied with animal ethics review standards (Animal License: SCXK (Beijing) 2016-0006; approved by the Institutional Animal Care and Use Committee of the Institute of Basic Medical Sciences, Chinese Academy of Medical Sciences, Animal Welfare Assurance Number: ACUC-A02-2014-007).

Blood Biochemical Analysis

To assess model progression and blood changes during the inflammatory-cancer transition, blood samples were collected from the abdominal aorta (2ml) under anesthesia with 2% pentobarbital sodium (0.2ml/100g) before DEN injection (week 0) and at weeks 4, 12, 16, and 18. Serum was obtained by centrifugation at 3000rpm for 10 minutes at 4℃. Levels of alanine aminotransferase (ALT), aspartate aminotransferase (AST), alkaline phosphatase (ALP), total protein (TP), and albumin (ALB) were measured.

Histopathological Analysis

Following blood collection, rats underwent cardiac perfusion. A needle was inserted from the left ventricular apex into the aorta, and physiological saline was rapidly perfused while a small incision was made in the right atrial appendage. After approximately 60ml of saline was perfused and the outflow became colorless, 4% paraformaldehyde was substituted. The liver was examined macroscopically, and liver tissue was collected for HE sectioning. Pathological sections were observed using Image Scope software to evaluate disease progression in the liver cancer-inflammatory cancer model.

Urine Collection and Sample Processing

Urine Collection: Urine was collected weekly, six days after each intraperitoneal DEN injection and before the next injection to minimize drug effects on urinary proteins. Each rat was placed in a metabolic cage overnight for 10-hour urine collection without food or water. Collected urine was immediately stored at -80℃ for subsequent analysis.

Urinary Protein Extraction and Digestion: Urine was centrifuged at 12,000g for 40 minutes at 4℃ to obtain the supernatant. Supernatant (500 l aliquots) was transferred to new EP tubes, and pre-cooled ethanol was added at a 1:3 ratio (supernatant:ethanol), mixed thoroughly, and stored overnight at -20℃ for 12 hours. The solution was then centrifuged at 12,000g for 30 minutes at 4℃, the supernatant was discarded, and the pellet was dried with cold air from a hair dryer. Lysis buffer (37.5 l) was added, mixed until no precipitate remained, and centrifuged again at 12,000g for 30 minutes at 4℃. The supernatant was transferred to new EP tubes and stored at -80℃. Protein concentration was determined using the Bradford method after resuspension.

For enzymatic digestion, the FASP method was employed [10]. Briefly, 100 g of urinary protein was loaded onto a 10kD ultrafiltration tube (Pall, Port Washington, NY, USA), washed twice with UA solution (8mol/L urea, 0.1mol/L Tris-HCl, pH8.5) and 25 mmol/L NH4HCO3 solution. Trypsin (Trypsin Gold, Promega, Fitchburg, WI, USA) was added at a 1:50 enzyme-to-protein ratio for overnight digestion at 37℃. Peptides were collected by centrifugation, desalted using HLB solid-phase extraction columns (Waters, Milford, MA), vacuum-dried, and stored at -80℃.

LC-MS/MS Analysis: Digested samples were resuspended in 0.1% formic acid and diluted to 0.5 g/ L. A pooled peptide sample was prepared from each sample and fractionated using a high pH reversed-phase peptide separation kit (Thermo Fisher Scientific). The pooled peptide sample was loaded onto a column and eluted with an acetonitrile gradient, collecting ten fractions by centrifugation. Fractions were vacuum-dried and resuspended in 0.1% formic acid. iRT synthetic peptides (Biognosis) were added to each fraction and individual sample at a 10:1 volume ratio.

Data acquisition was performed using an EASY-nLC 1200 ultra-high performance liquid chromatography system coupled to an Orbitrap Fusion Lumos high-resolution mass spectrometer. Peptides dissolved in 0.1% formic acid were loaded onto a pre-column (75 µm$\times 2cm, 3m, C18, 100) and separated on a reversed-phase analytical column (50m\times$250mm, 2µm, C18, 100Å) with a 4%-35% gradient of mobile phase B (80% acetonitrile + 0.1% formic acid + 20% water) at a flow rate of 300nL/min for 90 minutes. For automated and sensitive signal processing, a calibration kit (iRT kit, Biognosys, Switzerland) was used at 1:20 v/v concentration across all samples. Ten fractions were analyzed in DDA-MS mode with the following parameters: spray voltage 2.4kV, Orbitrap primary resolution 60,000, scan range 350-1550 m/z, secondary scan range 200-2000 m/z, resolution 30,000, isolation window 2Da, collision energy 30% HCD, AGC target 5e4, and maximum injection time 30ms. Raw files were processed using Proteome Discoverer 2.1 (PD, Thermo Fisher Scientific) for database searching and analysis.

Mass Spectrometry Data Processing: PD search results were used to establish DIA acquisition methods, with window width and quantity calculated based on m/z distribution density. Individual peptide samples were analyzed in DIA mode. Spectronaut X software was used for data processing and analysis, importing raw DIA files for database searching. High-confidence protein criteria were peptide q-value <0.01, with protein quantification based on the peak area of all fragment ions from secondary peptides.

Statistical Analysis: Missing values in mass spectrometry results were imputed using the KNN method [11], and CV screening (CV<0.3) was applied [12]. Independent sample t-tests were used for comparisons between each two groups. To minimize the impact of rat growth and development on urinary proteins, we employed adjacent time point comparisons: week 4 vs. week 0, week 8 vs. week 4, week 12 vs. week 8, week 16 vs. week 12, and week 18 vs. week 16. Differential proteins were screened using criteria of fold change FC$ 1.5 or FC $0.67, with P<0.05.

Functional Annotation of Differential Proteins: Differential proteins were analyzed for functional enrichment using the DAVID database (https://david.ncifcrf.gov/) [13] and IPA software (Ingenuity Systems, Mountain View, CA, USA), with significance threshold P<0.05.

Results

Rat Weight Changes

To broadly assess model progression, we recorded the weekly weight of 15 Wistar rats in the liver cancer-inflammatory cancer model. Weight changes followed expected patterns. Approximately 8-9 weeks after intraperitoneal injection, as hepatitis progressed, weight gain slowed. Around week 15, weight began to decline, corresponding to later histopathological results showing progression to the liver cancer stage (see Figure 1).

Blood Biochemistry Analysis

Blood biochemistry results revealed changes in five liver function parameters during the inflammatory-cancer transition. Alanine aminotransferase (ALT), influenced by hepatocellular membrane permeability, is generally associated with acute hepatitis and chronic cirrhosis. As shown in Figure 2a, ALT began to increase after week 12, indicating hepatocellular damage had affected the bloodstream. Aspartate aminotransferase (AST) elevation lagged behind ALT (Figure 2b), suggesting damage had progressed to the organelle level, with blood AST levels rising after week 16. The AST/ALT ratio showed corresponding changes (Figure 2c): initially decreasing as ALT increased during early hepatocellular injury, then rising as AST increased following mitochondrial damage. Between 0-12 weeks, hepatocytes began to sustain damage, with severe destruction occurring after week 16. Alkaline phosphatase (ALP) showed the most sensitive response, with significant elevation as early as week 4 that persisted throughout disease progression (Figure 2d). Despite liver damage, total protein (TP) and albumin (ALB) remained normal, likely due to homeostatic mechanisms (Figures 2e and 2f).

Macroscopic Liver Analysis

For direct model evaluation, we examined the surface appearance of livers from rats at different disease stages. Figures 3a-3d correspond to normal, hepatitis, cirrhosis, and liver cancer stages, respectively. Healthy livers appeared pale red, smooth, and soft. During hepatitis, livers became darker and firmer. In cirrhosis, the surface developed strong granularity with yellow-white spots. In liver cancer, dark red masses and diffuse gray-white nodules were visible.

Histopathological Analysis

Normal rat liver showed radially arranged hepatocyte cords with homogeneous red-stained cytoplasm, centrally located round nuclei, and no inflammatory cell infiltration in portal areas (Figure 4a). After 4 weeks, mild hepatitis with inflammatory cell infiltration in interstitial and portal areas was observed (Figure 4b), with some showing moderate hepatitis (Figure 4c). After 12 weeks, fibrous tissue proliferation, inflammatory infiltration, and pseudolobule formation indicated nodular cirrhosis (Figure 4d). At 16-18 weeks, large areas of tumor tissue with relatively well-differentiated, regularly arranged tumor cells and rare mitotic figures were observed, with extensive perivenous connective tissue proliferation and diffuse lymphocytic infiltration indicating early liver cancer (Figure 4e). In advanced liver cancer, tumor cells were poorly differentiated, irregularly arranged, with frequent mitotic figures and diffuse apoptosis, nuclear fragmentation, or dissolution (Figure 4f).

Urinary Proteome Analysis

Unsupervised Clustering Analysis: To better understand overall urinary proteome changes, we performed unsupervised clustering of all rats at all time points (Figure 5). The notation 1-0 represents rat #1 before DEN injection, 1-4 represents rat #1 at 4 weeks post-injection, and so forth. The clustering revealed that among 7 rats in the final liver cancer stage, 6 rats (1, 4, 5, 6, 7, 9) showed disease-associated urinary protein changes, while rat #3 exhibited significant individual variation. This highlights the importance of considering individual differences in disease models and the need for precision medicine tailored to each individual. Among the 6 disease-responsive rats, pre-injection week 0 samples clustered distinctly from other time points. Weeks 4-8 samples intermingled, likely reflecting the hepatitis stage where varying immune responses among rats led to different disease severity and progression rates. Week 16 samples clustered with either week 12 or week 18 samples, possibly due to individual variation in disease progression timing (some developing cirrhosis at week 12 vs. 16, or liver cancer at week 16 vs. 18). Overall, despite some intermingling of adjacent time points, unsupervised clustering successfully distinguished healthy, hepatitis, cirrhosis, and liver cancer stages while highlighting notable individual variation.

Differential Protein and Pathway Analysis: To minimize growth-related effects in self-controlled comparisons, we identified differential proteins in 7 rats using adjacent time point comparisons. Differential protein numbers at weeks 4, 8, 12, 16, and 18 are shown in Table 1 (specific UniProt information in Supplementary Table 1). Differential proteins were analyzed using Ingenuity Pathway Analysis software, with IPA pathways for different samples and time points summarized in Table 2 (partial pathways for 7 rats; complete pathways in Supplementary Table 2).

Statistical analysis of 7 rats identified 32 shared IPA pathways, most related to various stages of the inflammatory-cancer model. Among these, 18 pathways were liver disease-related, covering three main aspects: liver injury and inflammation, tumor development, and potential therapeutic targets. Five pathways involved liver damage, inflammation, and lesions: xenobiotic metabolism PXR signaling [14], α-adrenergic signaling [15], LXR/RXR activation [16], FXR/RXR activation [16], and iron homeostasis signaling [17]. Literature indicates PXR signaling and α-adrenergic signaling are associated with liver injury and inflammation, LXR/RXR and FXR/RXR activation relate to liver development, metabolism, and inflammation, and iron homeostasis signaling is linked to hepatic fibrosis. Most of these pathways were enriched at weeks 4 and 8. Nine pathways have been reported in literature as tumor-related, including SPINK1 pancreatic cancer pathway [18], NRF2-mediated oxidative stress response [19], glutathione-mediated detoxification [20], PXR/RXR activation [21], xenobiotic metabolism AHR signaling pathway [22], acute phase response signaling [23], gluconeogenesis I [24], complement system [25], and clathrin-mediated endocytosis signaling [26], all associated with tumor development including liver cancer. Four pathways were identified as

potential therapeutic targets, involving tumor growth, migration, cancer cell metabolism, and apoptosis: unfolded protein response [27], coagulation system [28], apoptosis signaling [29], and glycolysis I [30].

In summary, our results demonstrate that urinary proteomics can detect changes at each stage of the inflammatory-cancer model, with enriched biological processes documented in literature as hepatitis and liver cancer-related. Individual biological variation leads to different disease progression rates in carcinogenesis models.

References

[1] YouHe Gao. Urine—an untapped goldmine for biomarker discovery?[J]. Science China Life Sciences, 2013, 56(12).

[2] Thongboonkerd V, McLeish K R, Arthur J M, et al. Proteomic analysis of normal human urinary proteins isolated acetone precipitation or ultracentrifugation. Kidney Int, 2002, 62: 1461-1469.

[3] Yuhang Huan, Weiwei Qin, Youhe Gao. Factors to consider in the verification of urinary biomarkers[J]. Science China (Life Sciences), 2018, 61(10): 1283-1290.

[4] Tomasz P Radon1, Nathalie J Massat. Identification of a three-biomarker panel in urine for early detection of pancreatic adenocarcinoma[J]. Clin Cancer Res. 2015 August 1; 21(15): 3512–3521.

[5] Virginia Urquidi1, Mandy Netherton. Urinary mRNA biomarker panel for the detection of urothelial carcinoma[J]. Oncotarget, 2016. Vol. 7, No. 25.

[6] Youhe Gao. Roadmap to the Urine Biomarker Era[A]. National Foreign Experts Bureau Foreign Talent Resources General Database Dalian Talent Subdatabase, Biotech International Conference (Dalian) Co., Ltd. Proceedings of the 1st International Urology Conference 2015[C]. National Foreign Experts Bureau Foreign Talent Resources General Database Dalian Talent Sub-database, Biotech International Conference (Dalian) Co., Ltd.: Biotech International Conference (Dalian) Co., Ltd., 2015: 1.

[7] Liu Huang, Liu Jing. Research progress in animal models of liver cancer[J]. World Chinese Journal of Digestology, 2011, 19(12): 1275-1278.

[8] Dr. D. Max Parkin MD, Mr. Freddie Bray, Mr. J. Ferlay, Dr. Paola Pisani PhD. Global Cancer Statistics, 2002[J]. CA: A Cancer Journal for Clinicians, 2005, 55(2).

[9] Philippa Newell, Augusto Villanueva, Scott L. Friedman, Kazuhiko Koike, Josep M. Llovet. Experimental models of hepatocellular carcinoma[J]. Journal of Hepatology, 2008, 48(5).

[10] Wisniewski, J.R., et al., Universal sample preparation method for proteome analysis. Nat Methods, 2009. 6(5): p. 359-62.

[11] Armitage, E.G., et al., Missing value imputation strategies for metabolomics data. Electrophoresis, 2015. 36(24): p. 3050-60.

[12] Wang, S., et al., NAguideR: performing and prioritizing missing value imputations for consistent bottom-up proteomic analyses. Nucleic Acids Res, 2020. 48(14): p. e83.

[13] Huang da, W., B.T. Sherman, and R.A. Lempicki, Systematic and integrative analysis of large gene lists using DAVID bioinformatics resources. Nat Protoc, 2009. 4(1): p. 44-57.

[14] Mutual repression between steroid and xenobiotic receptor and NF- B signaling pathways links xenobiotic metabolism and inflammation[J]. The Journal of Clinical Investigation, 2006, 116(8).

[15] Lin Jung-Chun, Peng Yi-Jen, Wang Shih-Yu, Lai Mei-Ju, Young Ton-Ho, Salter Donald M, Lee Herng-Sheng. Sympathetic Nervous System Control of Carbon Tetrachloride-Induced Oxidative Stress in Liver through α-Adrenergic Signaling.[J]. Oxidative medicine and cellular longevity, 2016, 2016.

[16] Yin and Yang Regulation of Liver X Receptor α Signaling Control of Cholesterol Metabolism by Poly(ADP-ribose) polymerase 1.[J]. International journal of biological sciences, 2020, 16(15).

[17] Changying Li, Yingying Liu, Zheng Dong, Ming Xu, Ming Gao, Min Cong, Sijin Liu. TCDD promotes liver fibrosis through disordering systemic and hepatic iron homeostasis[J]. Journal of Hazardous Materials, 2020, 395(prepublish).

[18] Zhao Na, Zheng Yang, Chen Lili, Jing Donghui, Wang Huaqing. Clinical value and application of SPINK1 as a tumor marker[J]. International Journal of Oncology, 2020, 47(07): 414-418.

[19] Liu Qian, Zhang Hao, Smeester Lisa, Zou Fei, Kesic Matt, Jaspers Ilona, Pi Jingbo, Fry Rebecca C. The NRF2-mediated oxidative stress response pathway is associated with tumor cell resistance to arsenic trioxide across the NCI-60 panel.[J]. BMC medical genomics, 2010, 3(1).

[20] Ding Yiming, Dai Yujie, Wu Mengqi, Li Linlin. Glutathione-mediated nanomedicines for cancer diagnosis and therapy[J]. Chemical Engineering Journal, 2021, 426.

[21] Guo Enshuang. Study on the mechanism of HBx intervention in PXR/RXRα regulation of CYP3A4 expression in HBV-induced hepatocellular carcinoma[D]. Southern Medical University, 2014.

[22] Dietrich C, Kaina B. The aryl hydrocarbon receptor (AhR) in the regulation of cell–cell contact and tumor growth[J]. Pergamon Press, 2010.

[23] Rania Dayoub, Leonhard Buerger, Sara Ibrahim, Michael Melter, Thomas S. Weiss. Augmenter of liver regeneration (ALR) exhibits a dual signaling impact on hepatic acute-phase response[J]. Experimental and Molecular Pathology, 2017, 102(3).

[24] Roh M S, Ekman L, Jeevanandam M, Brennan M F. Gluconeogenesis in tumor-influenced hepatocytes.[J]. Surgery, 1984, 96(2).

[25] Zhang Lingling, Xu Weiran, Liang Jun. New progress in the relationship between complement activation and tumor immunity[J]. Chinese Journal of Laboratory Medicine, 2017, 40(09): 664-666.

[26] Wang Xiaowei, Qiu Yuhan, Wang Mengyan, Zhang Conghui, Zhang Tianshu, Zhou Huimin, Zhao Wenxia, Zhao Wuli, Xia Guimin, Shao Rongguang. Endocytosis and Organelle Targeting of Nanomedicines in Cancer Therapy.[J]. International journal of nanomedicine, 2020, 15.

[27] Obacz J, Avril T, Camila Rubio Patio, et al. Regulation of tumor–stroma interactions by the unfolded protein response[J]. The FEBS Journal, 2019, 286(2).

[28] Magnus N, D'Asti E, Meehan B, et al. Oncogenes and the coagulation system - Forces that modulate dormant and aggressive states in cancer[J]. Thrombosis Research, 2014, 133 Suppl 2(Suppl): S1-9.

[29] Fulda Simone, Debatin Klaus-Michael. Apoptosis signaling in tumor therapy.[J]. Annals of the New York Academy of Sciences, 2004, 1028.

[30] Ganapathy-Kanniappan Shanmugasundaram. Targeting tumor glycolysis by a mitotropic agent.[J]. Expert opinion on therapeutic targets, 2016, 20(1).

Author Contributions

Wang Yunlong and Gao Youhe: Conceived the research idea and designed the study;
Wang Yunlong: Performed the experiments;
Wang Yunlong: Analyzed the data;
Wang Yunlong: Drafted the manuscript;
Gao Youhe: Revised the final version of the manuscript.

Figures

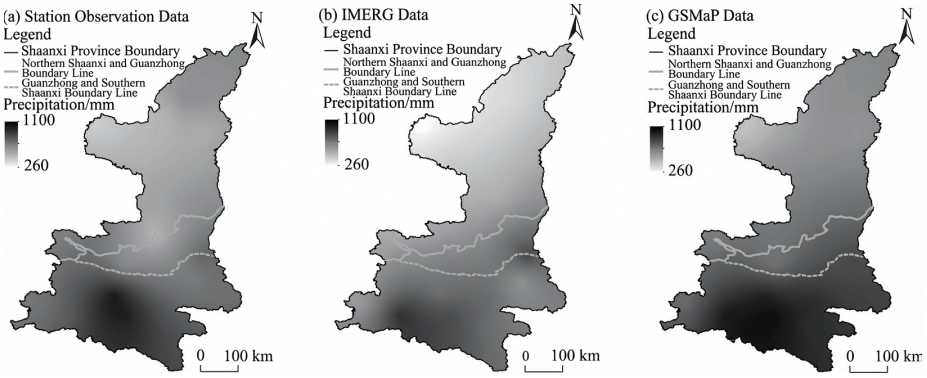

Figure 1: Figure 2

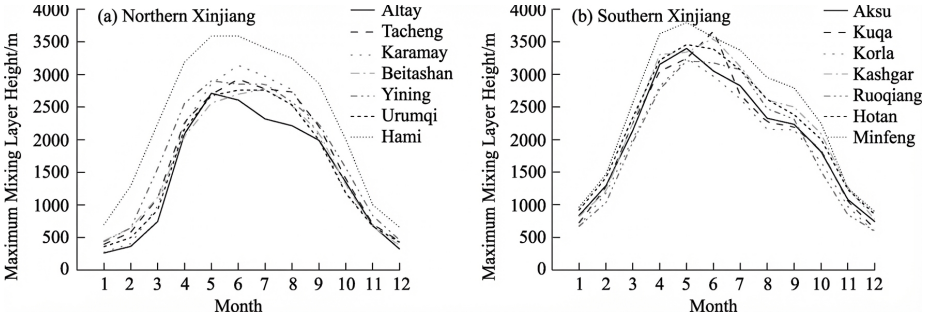

Figure 2: Figure 3

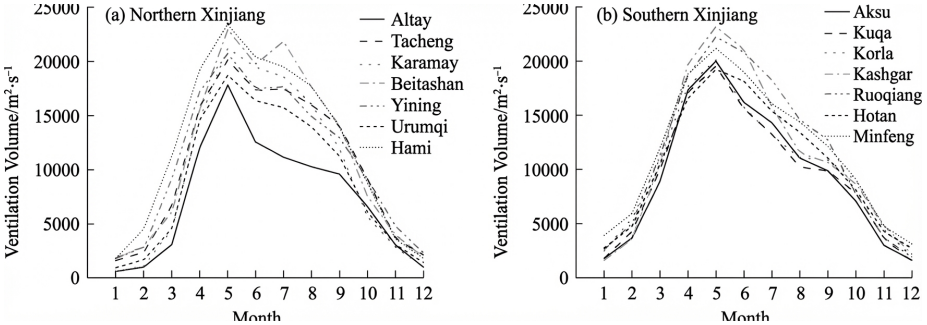

Figure 3: Figure 5